

Article

p66 α Suppresses Breast Cancer Cell Growth and Migration by Acting as Co-Activator of p53

Qun Zhang^{1,2}, Yihong Zhang^{1,2}, Jie Zhang^{1,2}, Dan Zhang^{1,2}, Mengying Li^{1,2}, Han Yan^{1,2}, Hui Zhang^{1,2}, Liwei Song^{3,4}, Jiamin Wang^{1,2}, Zhaoyuan Hou^{1,2}, Yunhai Yang^{3,*} and Xiuqun Zou^{1,2,*}

- ¹ Hongqiao International Institute of Medicine, Tongren Hospital/Faculty of Basic Medicine, Shanghai Jiaotong University School of Medicine, Shanghai 200025, China; zhang.qun@sjtu.edu.cn (Q.Z.); Zhang_yihong2022@163.com (Y.Z.); zhangjie0307zjzz@sjtu.edu.cn (J.Z.); zhangdan_0117@163.com (D.Z.); limengying37@126.com (M.L.); Yanhan1108@126.com (H.Y.); zanghuier@outlook.com (H.Z.); jesuisjm@163.com (J.W.); houzy@sjtu.edu.cn (Z.H.)
- ² Shanghai Key Laboratory for Tumor Microenvironment and Inflammation, Department of Biochemistry & Molecular Cellular Biology, Shanghai Jiaotong University School of Medicine, Shanghai 200025, China
- ³ Shanghai Pulmonary Tumor Medical Center, Shanghai Chest Hospital, Shanghai 200025, China; songliwei_2011@163.com
- ⁴ Naruibo Biomedical Technology Corporation Limited, Linyi 277700, China
- * Correspondence: docyuh@163.com (Y.Y.); queensmile@sjtu.edu.cn (X.Z.)

Abstract: p66 α is a GATA zinc finger domain-containing transcription factor that has been shown to be essential for gene silencing by participating in the NuRD complex. Several studies have suggested that p66 α is a risk gene for a wide spectrum of diseases such as diabetes, schizophrenia, and breast cancer; however, its biological role has not been defined. Here, we report that p66 α functions as a tumor suppressor to inhibit breast cancer cell growth and migration, evidenced by the fact that the depletion of p66 α results in accelerated tumor growth and migration of breast cancer cells. Mechanistically, immunoprecipitation assays identify p66 α as a p53-interacting protein that binds the DNA-binding domain of p53 molecule predominantly via its CR2 domain. Depletion of p66 α in multiple breast cells results in decreased expression of p53 target genes, while over-expression of p66 α results in increased expression of these target genes. Moreover, p66 α promotes the transactivity of p53 by enhancing p53 binding at target promoters. Together, these findings demonstrate that p66 α is a tumor suppressor by functioning as a co-activator of p53.

Keywords: p66 α ; p53; cell growth; metastasis; migration; breast cancer



Citation: Zhang, Q.; Zhang, Y.; Zhang, J.; Zhang, D.; Li, M.; Yan, H.; Zhang, H.; Song, L.; Wang, J.; Hou, Z.; et al. p66 α Suppresses Breast Cancer Cell Growth and Migration by Acting as Co-Activator of p53. *Cells* **2021**, *10*, 3593. <https://doi.org/10.3390/cells10123593>

Academic Editors: Ming Luo and Alexander E. Kalyuzhny

Received: 12 October 2021
Accepted: 16 December 2021
Published: 20 December 2021

Publisher's Note: MDPI stays neutral with regard to jurisdictional claims in published maps and institutional affiliations.



Copyright: © 2021 by the authors. Licensee MDPI, Basel, Switzerland. This article is an open access article distributed under the terms and conditions of the Creative Commons Attribution (CC BY) license (<https://creativecommons.org/licenses/by/4.0/>).

1. Introduction

p66 α (GATA zinc finger domain-containing protein 2A, GATAD2A) and p66 β (GATA zinc finger domain-containing protein 2B, GATAD2B) are two highly related 66-kDa proteins identified as MBD2 (methyl-CpG binding domain protein 2) interacting proteins in yeast two-hybrid screening assays [1]. They share two conserved domains: the N-terminal CR1 domain and the C-terminal GATA zinc finger-containing CR2 domain [1].

GATA zinc fingers comprise general configurations of Cys-X2-Cys-X17-Cys-X2-Cys and can specifically bind the consensus sequence A/T(GATA)A/G in target promoters to modulate gene transcription [2–5]. The three-dimensional structure of the zinc fingers in GATA-1 has revealed that the core DNA-binding domain contains two anti-parallel beta sheets and an alpha helix followed by a loop, which is the structural basis for interacting with DNA grooves [6]. The classical GATA transcription factors contain one or two conserved zinc fingers, and all vertebrate GATA transcription factors have two zinc fingers [5]. The C-terminal zinc finger specifically recognizes the consensus sequence in the target promoters, and the N-terminal zinc finger predominantly interacts with the partner proteins such as the FOG family proteins to stabilize the DNA-protein complex [7–9]. However,

there is only one GATA zinc finger in p66 α /p66 β , which has not been demonstrated to be capable of binding DNA.

p66 α /p66 β were identified as essential components of the highly conserved, ATP-dependent, chromatin remodeling NuRD (Nucleosome Remodeling and Deacetylase) complex [10], which contains CpG-binding proteins MBD2/3, ATP-dependent remodeling enzymes CHD3/4, histone deacetylases HDAC1/2, p66 α and p66 β , histone chaperones RbAp46/48, and DNA-binding proteins MTA1/2/3 [11]. The NuRD complex dominates a transcriptional repression process of DNA methylation depending on its nucleosome remodeling activity and participates in various cellular functions such as DNA damage repairing and mRNA splicing [12–20]. p66 α is shown to be necessary for targeting the NuRD complex to specific nuclear loci and mediating histone tail interaction [10,12]. The interaction between the p66 α CR1 domain and MBD2 coiled-coiled domain is essential for the recruitment of CHD4 to the NuRD complex, and its deficiency would disrupt the repressive function of the complex [1,10,21]. ZMYND8 can recruit the NuRD complex to the DNA breaks via p66 α and subsequently promote DNA repair by homologous recombination [22]. Moreover, phosphorylated p66 α can recruit Suv39h1 and HDAC2 to establish repressive histone marks that affect the splicing process of *Neurexin-1* mRNA, leading to changed connectivity of the activated neurons [12]. Most recently, p66 α mutants were determined to impair the recruitment of CHD4 to the MBD2-NuRD complex, leading to disturbed silencing effects on γ -globin and an elevated fetal hemoglobin (HbF) level in patients with β -thalassemia [13,23]. Moreover, SUMO modification of p66 α can enhance the transcriptional repression of the NuRD complex by promoting protein interactions within the complex [24]. Inhibition of p66 α promotes iPSC reprogramming by disrupting Mbd3/NuRD repressive activity on the pluripotency circuitry [20]. Biologically, p66 α is expressed during early embryonic development, and its genetic deletion leads to a lethal embryo phenotype in mice [25,26].

Studies have shown that p66 α is involved in tumor development. For example, depletion of p66 α results in suppressed cell proliferation in thyroid cancer cells [17], and p66 α interacts with STAT3 to suppress its phosphorylation and K63 ubiquitination in myeloid-derived suppressor cell (MDSC), resulting in the reduced differentiation and the repressed immune suppressive function of MDSCs [27]. By genome-wide meta-analyses, p66 α has been identified as a risk gene for breast cancer [28,29]. However, the precise role of p66 α in breast cancer remains to be elucidated.

p53 is one of the most studied classical tumor suppressors [30–32]. When cells are insulted by stresses such as DNA damage, hypoxia, and oncogene activation, p53 is activated to transcriptionally regulate genes involved in the cell cycle, cell death, cell migration, and angiogenesis, which contribute to the maintenance of genomic stability, suppression of cell growth and tumor development [33–37]. However, *TP53* is one of the most altered genes in cancer and is mutated in about 23% of breast cancer samples [38]. The DNA-binding domains of p53 are a hot spot bearing many point mutations [39]. Some point mutations, such as mutants at amino residues R248, R273, and R280, have been classified as “contact mutants” since they directly impact contact between p53 and the target DNA sequences [38]. However, some p53 mutants still retain function as sequence-specific transcription factors, showing an altered but not totally eliminated ability to transactivate target promoters [40–42]. Thus, a single residue alteration in p53 can trigger a considerable diversity in the response profile of different response elements [40,43–47].

In this study, we report that p66 α suppresses the growth and migration of breast cancer cells by interacting with p53 to enhance the binding activity of p53 at target promoters and increase the expression of p53 target genes. Moreover, p66 α can also promote the transcriptional activation function of the p53 R280K found in MDA-MB-231 cells.

2. Materials and Methods

2.1. Plasmids

The pcDNA-Flag-p66 α plasmid was kindly gifted by Dr. Reiner Renkawitz, Genetisches Institut Justus-Liebig-Universität. The HA-p66 α and pCDH-Flag-p66 α plasmids were subcloned into pCMV5-HA-vecor and pCDH-CMV-MCS-EF1-Puro-vector, respectively. The deletion mutant plasmids Flag-p66 α -CR1 and Flag-p66 α -CR2 were subcloned into pCMV4-Flag-vector by PCR method between *Bam*H I and *Eco*R I restriction enzyme sites. PCR amplification was carried out using Phanta Max Super-Fidelity Polymerase (P505-d1, Vazyme, Piscataway, NJ, USA). The GFP-p53 plasmid was kindly gifted by Pf. Jing Yi, Shanghai Jiaotong University School of Medicine. The Flag-p53 and its truncation mutant plasmids were subcloned into pCDNA3.1-Flag-vector and pGEX-4T1-vector by PCR method between *Bam*H I and *Eco*R I restriction enzyme sites. pLKO.1-p66 α shRNA plasmids were generated with the oligonucleotides 5'-TTCTCTCAGAATGTCTGCCGG-3' and 5'-CCGGCAGACATTCTGAGAGAA-3', which target the coding region of the p66 α transcript. The promoter DNA sequences of human *BAX* (−478 to +12 bp) and *NOXA* (−471 to −1 bp) were subcloned into pGL3-basic-vector to create the corresponding luciferase reporters.

2.2. Cell Culture, Transfections, and Viral Infection

HEK-293T, MDA-MB-231, MCF-7 cells were cultured in Dulbecco's modified Eagle's medium (DMEM) supplemented with 10% fetal bovine serum (FBS), penicillin (50 U/mL)/streptomycin (50 μ g/mL). MCF-10A cells were cultured in Dulbecco's Modified Eagle Medium/Nutrient Mixture F-12 supplemented with 5% horse serum, EGF (20 ng/mL), insulin (10 μ g/mL), hydrocortisone (0.5 μ g/mL), cholera toxin (100 ng/mL), and penicillin (50 U/mL)/streptomycin (50 μ g/mL). All of the cells were cultured at 37 °C under 5% CO₂ in a humidified chamber.

For transient transfection, plasmids were transiently transfected into cells at approximately 70% confluence using PEI reagent (#23966-2, polysciences, Warrington, PA, USA) according to the manufacturer's instructions. After 48 h of transfection, cells were harvested.

The stable cells were established via the viral infection method. For lentivirus packages, indicated plasmids were transfected into HEK-293T cells according to the transient transfection method. The supernatants containing viruses were collected at 48 h and 72 h after transfection and used to infect target cells. Twenty-four hours post-infection, puromycin (1 μ g/mL for MDA-MB-231 and MCF-10A cells, 2 μ g/mL for MCF-7 cells) was added to select the stable cells for 5 days.

2.3. Western Blot, Immunofluorescence, Co-IP and GST Pull Down

Western blotting and immunofluorescence assays were carried out as described [48,49]. Plasmids encoding Flag-p66 α , GFP-p53 or HA-p66 α , Flag-p53 were transiently transfected into HEK-293T cells, and 24 h after transfection, cells were lysed in the cell lysis buffer containing 20 mM Tris (pH 7.5), 150 mM NaCl, 2.5 mM EDTA, DTT, and protease inhibitor mixture.

GST-p53 and its truncation mutant proteins were expressed in *E. coli* BL21 and purified by using GST beads (17-0756-01, GE Healthcare, Little Chalfont, Buckinghamshire, UK).

The antibodies used were as follows: mouse anti-Flag antibody (F3165, Sigma-Aldrich, St. Louis, MO, USA), rabbit anti-Flag antibody (F7425, Sigma-Aldrich, St. Louis, MO, USA), rabbit anti-GST antibody (#2622, Cell Signaling Technology, Danvers, MA, USA), mouse anti-HA antibody (901503, BioLegend, San Diego, CA, USA), rabbit anti-GATAD2A (H-162) antibody (sc-134712, Santa Cruz Biotechnology, Santa Cruz, CA, USA), mouse anti-p53 (DO-1) antibody (sc-126, Santa Cruz Biotechnology, Santa Cruz, CA, USA), rabbit anti-p53 (7F5) antibody (#2527, Cell Signaling Technology, Danvers, MA, USA), anti- β -actin antibody (66009-1-Ig, Proteintech, Chicago, IL, USA), mouse GFP-antibody (50430-2-AP, Proteintech, Chicago, IL, USA), Alexa Fluor 488 Donkey anti-Mouse IgG (A-21202, Invitrogen, Carlsbad,

CA, USA), Alexa Fluor 568 Donkey anti-Rabbit IgG (A-10042, Invitrogen, Carlsbad, CA, USA), Alexa Fluor 568 Rabbit anti-Mouse IgG (A-11061, Invitrogen, Carlsbad, CA, USA).

2.4. Reverse Transcription PCR (RT-PCR) and Quantitative Real-Time PCR (qRT-PCR)

Total RNA from stable cells was extracted using the TRIzol reagent (15596026, Life Technologies, Carlsbad, CA, USA) according to the manufacturer's instructions. Reverse transcription procedure was described previously; three micrograms of the treated total RNA were used for cDNA synthesis in a 20 μ L reaction using SuperScript II reverse transcriptase (18064022, Invitrogen, Carlsbad, CA, USA) [48–50].

qRT-PCR was performed using Hieff SYBR Green Master Mix (11201ES03, Yeasen Biotech, Shanghai, China), and reactions were performed on Roche LightCycler[®] 480 II Real-Time PCR System. Data were acquired and analyzed using the $2^{-\Delta\Delta CT}$ method with ACTIN as an endogenous control. Probes and primers used in qRT-PCR are listed in Table S1 (Supplementary Material).

2.5. Chromatin Immunoprecipitation (ChIP)

ChIP assays were carried out in MDA-MB-231-Luc shVector and shp66 α cells. The cells were grown in 100 mm plates to 90% confluence and fixed by 1% formaldehyde for 10 min in the cell culture incubator. The cross-linking reaction was stopped by 0.125 M glycine in $1 \times$ PBS at room temperature for 5 min. Cells were harvested, washed, and lysed in the ChIP lysis buffer containing 150 mM NaCl, 50 mM Tris-HCl (pH7.5), 5 mM EDTA, NP-40 (0.5% vol/vol), TritonX-100 (1.0% vol/vol). The chromatin was sonicated to fragments ranging from 300–800 bp in size. Immunoprecipitation was performed using the antibody against p53 (mouse, DO-1, Santa Cruz Biotechnology, Santa Cruz, CA, USA), mouse normal IgG (sc-2025, Santa Cruz Biotechnology, Santa Cruz, CA, USA). The immunoprecipitated DNAs were amplified by qRT-PCR. Primers used for ChIP qRT-PCR were listed in Table S2 (Supplementary Material).

2.6. Luciferase Reporter Assay

Luciferase reporter assay was performed in HEK-293T cells. After 24 h transfection, cells were harvested in luciferase lysis buffer. Firefly luciferase activity (MA0519, Meilunbio, Dalian, China) and β -galactosidase activity (631712, Takara, Tokyo, Japan) were measured using the Commercial reagents according to the manufacturer's instructions.

2.7. Cell Counting Assay

Cells (3000 per well) were plated in a 96-well plate containing 100 μ L/well medium, and cell counting assays were performed according to the manufacturer's instructions of Cell Counting Kit-8 (CK04, Dojindo, Shanghai, China). Absorbance at 450 nm was quantified at different time points using the Multiskan MK3 microplate reader (Thermo Fisher Scientific, Waltham, MA, USA). The cell growth curve was drawn with the Graphpad Prism.

2.8. Cell Migration Assay

Migration assays were performed as described previously [50]. After being starved for about 12 h, stable cells were harvested using trypsin and counted. A total of 5×10^4 cells were resuspended in the serum-free medium and placed in the upper 8 μ m pore transwell filters (3495, Corning Incorporated, Corning, NY, USA). Complete DMEM medium was added to the bottom chamber as attractants. The chamber was incubated at 37 $^{\circ}$ C and in a 5% CO₂ atmosphere for 18 hours. The cells were fixed with 4% poly-formaldehyde for 15 min, and cells were stained with Coomassie Brilliant Blue (G250) for 30 min. Non-migrated cells on the upper side of the filter were removed with a cotton swab. The chamber was washed with PBS 2–3 times and dried up at 37 $^{\circ}$ C [50]. The migrated cells on the bottom of filter were quantified by counting nine randomly chosen fields (20 \times) using microscopy in each well. Experiments were repeated in triplicates.

2.9. Immunoprecipitation Mass Spectrometry

A total of 4×10^8 cells were lysed in lysis containing 20 mM Tris-HCl (pH 8.0), 150 mM NaCl, 2.5 mM EDTA, 0.5% NP-40, 0.2 mM PMSF, and 0.1 mM cocktail. Cell lysates were precleared with the protein A-agarose beads (sc-2003, Santa Cruz Biotechnology, Santa Cruz, CA, USA) for 2 h and then incubated with the anti-Flag agarose M2 beads (F2426, Sigma-Aldrich, St. Louis, MO, USA) at 0.5 mL of beads per 100 mg of cell lysate for 2 h to overnight with rotation. The M2 beads were washed four times with buffer BC500 containing 20 mM Tris-HCl (pH 7.8), 500 mM KCl, 0.2 mM EDTA, 10% glycerol, 10 mM mercaptoethanol, 0.2% NP-40, 0.2 mM PMSF, and 0.1 mM cocktail. The protein complex was eluted with the Flag peptides (Sigma-Aldrich, St. Louis, MO, USA) at 0.2 mg/mL in buffer TBS containing 20 mM Tris-HCl (pH 7.8), 50 mM NaCl, 0.2 mM PMSF, and 0.1 mM cocktail. The eluted proteins were resolved on 4 to 12% sodium dodecyl sulfate-polyacrylamide gel electrophoresis gels for Western blotting and silver and colloidal staining analyses. The proteins located between 40-kDa and 55-kDa were excised from the gels and identified by standard mass spectrometry.

2.10. Subcutaneous Xenograft Assay

Female BALB/c nude mice were purchased from SLAC Laboratory Co. Ltd. (Shanghai, China) and divided into two groups randomly. The total number of 2×10^6 (in 100 μ L of PBS per mouse) luciferase-expressing MDA-MB-231 cells with or without p66 α depletion cells was injected into 6-week-old nude mice subcutaneously per group ($n = 10$). Three weeks after inoculation, the mice were euthanized and the tumors were dissected and fixed in 4% paraformaldehyde. The volume of tumors was estimated according to the formula $V = 0.52 \times L \times W^2$.

2.11. Lung Metastasis Assay and Hematoxylin and Eosin (H&E) Staining

Female BALB/c nude mice were purchased from SLAC Laboratory Co. Ltd. (Shanghai, China) and divided into two groups randomly. To analyze lung metastasis, a total number of 2×10^6 (in 100 μ L of PBS per mouse) luciferase-expressing MDA-MB-231 cells with or without p66 α depletion cells were injected into the tail vein of 6-week-old female mice ($n = 10$ for each group). After inoculation, bioluminescence imaging of metastatic tumors was carried out using Xenogen IVIS Imaging System every two weeks.

For H&E staining, the mice were euthanized and the lungs were dissected and fixed in 4% paraformaldehyde for 48 h. Samples were dehydrated in graded ethanol series followed by xylene. Subsequently, samples were then embedded in paraffin, sectioned onto slides (5 mm thick), and dried. Slides were deparaffinized using the standard procedure (xylene \times 2 washes, 100% ethanol \times 2 washes, 95% ethanol, 70% ethanol, 50% ethanol) and stained with H&E (HT110132, Sigma-Aldrich, St. Louis, MO, USA).

2.12. Survival Analysis and Correlation Analysis

The survival analyses of p66 α and p53 were generated from Kaplan-Meier plots online tools, which are capable of assessing the effect of 54 k genes (mRNA, miRNA, protein) on survival in 21 cancer types including breast cancer. The patient samples are split into two groups according to the expression level of p66 α or p53. The two patient cohorts are compared by the Kaplan-Meier survival plot, and the hazard ratio with 95% confidence intervals and log-rank p value is calculated. (<http://kmplot.com>, accessed on 3 December 2021)

The correlation analysis of p66 α and p53 in breast cancer was generated with the online tools based on the TCGA database GEPIA (<http://gepia.cancer-pku.cn/>, accessed on 3 December 2021).

2.13. Statistical Analysis

Data presented as mean \pm SD were analyzed by the independent Student's t test.

3. Results

3.1. *p66 α Inhibits Breast Cancer Cell Growth*

To examine if p66 α participates in breast-cancer-relevant biological processes, we first performed extensive bioinformatics analyses to determine if there is a correlation between p66 α expression level and the clinical outcome in breast cancer patients. We found that patients with the high level of p66 α expression showed a better overall survival outcome (Figure 1A). This observation prompted us to examine the effect of p66 α on breast cancer cell growth. First, p66 α was depleted in MCF-7 cells by using specific targeting shRNAs (Figure 1B), and the cell growth rate was examined by CCK8 assays. Notably, depletion of p66 α increased the growth of MCF-7 cells significantly (Figure 1C). Conversely, ectopic expression of p66 α inhibited the growth of MCF-7 cells (Figure 1D,E). Similarly, knockdown of p66 α in MDA-MB-231 resulted in increased cell growth (Figure 1F,G), while overexpression of p66 α significantly inhibited cell growth (Figure 1H,I). Similar results were also observed in MCF-10A, which is classified as a normal breast cell line (Figure S1A,B). Next, we subcutaneously injected the MDA-MB-231-Luc-shp66 α or MDA-MB-231-Luc-shVector cells into nude mice, which were euthanized to dissect the tumors 18 days post-injection. The tumor sizes were measured and showed that the volume of the tumors in the knockdown p66 α group was remarkably larger than those in the control group (Figure 1J,K), indicating that depletion of p66 α enhances the tumor cell growth.

3.2. *p66 α Suppresses Breast Cancer Cell Migration and Metastasis*

To determine the role of p66 α in breast cancer cell migration, cells stably expressing shp66 α or vector were subjected to transwell assays. Depletion of p66 α expression markedly promoted cell migration in MCF-7 and MDA-MB-231 cells, respectively (Figure 2A,B,E,F). Conversely, ectopic expression of p66 α resulted in decreased cell migration in MCF-7 and MDA-MB-231 cells (Figure 2C,D,G,H). Consistent with these observations, over-expression of p66 α significantly inhibited cell migration in MCF-10A cells (Figure S1C,D). To expand these observations, we used the tail vein injection lung metastasis model to examine the impact of p66 α on tumor metastasis in vivo. MDA-MB-231-Luc-shp66 α cells and control cells were injected into the tail vein of the nude mice, and metastatic tumor nodules were recorded by in vivo imaging technology every other week (Figure 2I). The luciferase signal intensities of lung metastatic nodules were significantly increased in the shp66 α group compared with those in the control group (Figure 2J), and H&E staining assays revealed that the metastatic foci in the shp66 α group were dramatically increased in tissue sections of the lungs (Figure 2K,L). Taken together, these observations demonstrate that p66 α suppresses the migration and metastasis of breast cancer cells.

3.3. *p66 α Interacts with p53*

To investigate how p66 α elicits the suppressive effects on cell growth and migration, we performed an immunoprecipitation coupled mass spectrometry assay to explore p66 α -interacting proteins. We established HEK-293T cells stably expressing Flag- p66 α and performed affinity purification with Flag antibody. p53 was identified as a potential p66 α -interacting protein. To confirm the interaction between p66 α and p53, we first transiently co-expressed full-length p66 α and p53 in HEK-293T cells, and co-immunoprecipitations were performed. Indeed, p66 α robustly and reciprocally interacted with p53 in HEK-293T cells (Figure 3A,B). To further confirm that a p66 α -p53 interaction occurs within the endogenous proteins, whole-cell lysates prepared from HEK-293T-Flag- p66 α cells were used for immunoprecipitation with antibody against p66 α , and Western blotting assays showed that p66 α could co-elute with endogenous p53 protein (Figure 3C). Furthermore, indirect immunofluorescence staining showed that the two proteins co-existed in the nucleoplasm (Figure 3D). Collectively, these data suggest that p53 is a p66 α -interacting protein.

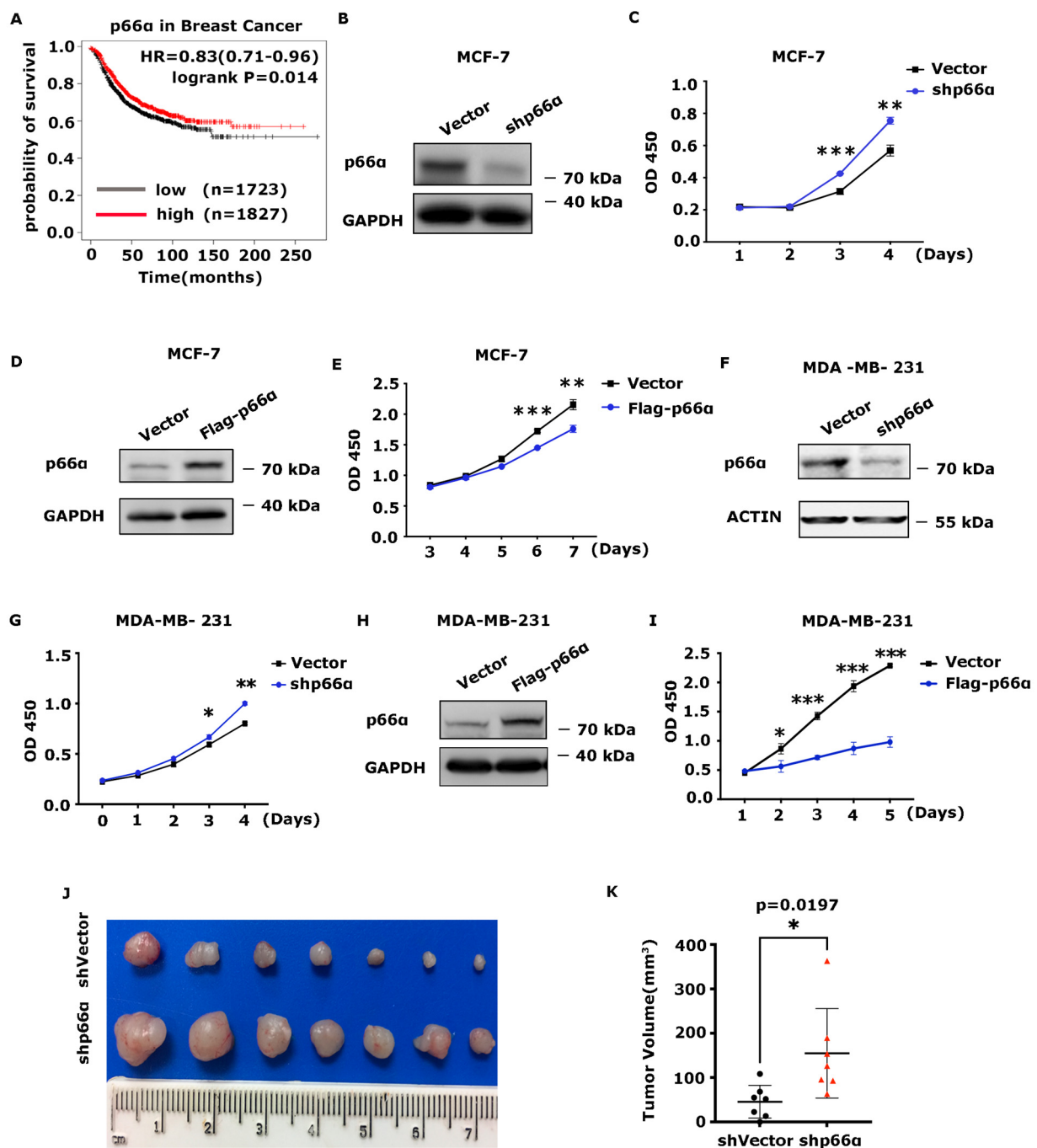


Figure 1. p66α inhibits breast cancer cell growth. (A) Kaplan-Meier plot of the relapse-free survival of patients with breast cancer stratified by p66α. (B) Western blot assays showed that p66α was effectively depleted in the MCF-7 cell line. (C) Cell growth curves of p66α knockdown MCF-7 cells and control cells. (D) Western blot assays showed that p66α was over-expressed in the MCF-7 cells. (E) Cell growth curves of MCF-7 cells overexpressing p66α or mock vector. (F) Western blot assays showed the depletion of p66α in the MDA-MB-231 cells. (G) The cell growth curves of p66α knockdown MDA-MB-231 cells and mock cells. (H) Western blot assays showed the expression of p66α in MDA-MB-231 cells. (I) The cell growth curves of MDA-MB-231 cells overexpressing p66α or mock control. (J) Tumor size of subcutaneous tumor formation assay. Knockdown of p66α in MDA-MB-231 cells promoted cell growth in vivo ($n = 7$). (K) statistical results of (J). * $p < 0.05$, ** $p < 0.01$, *** $p < 0.001$.

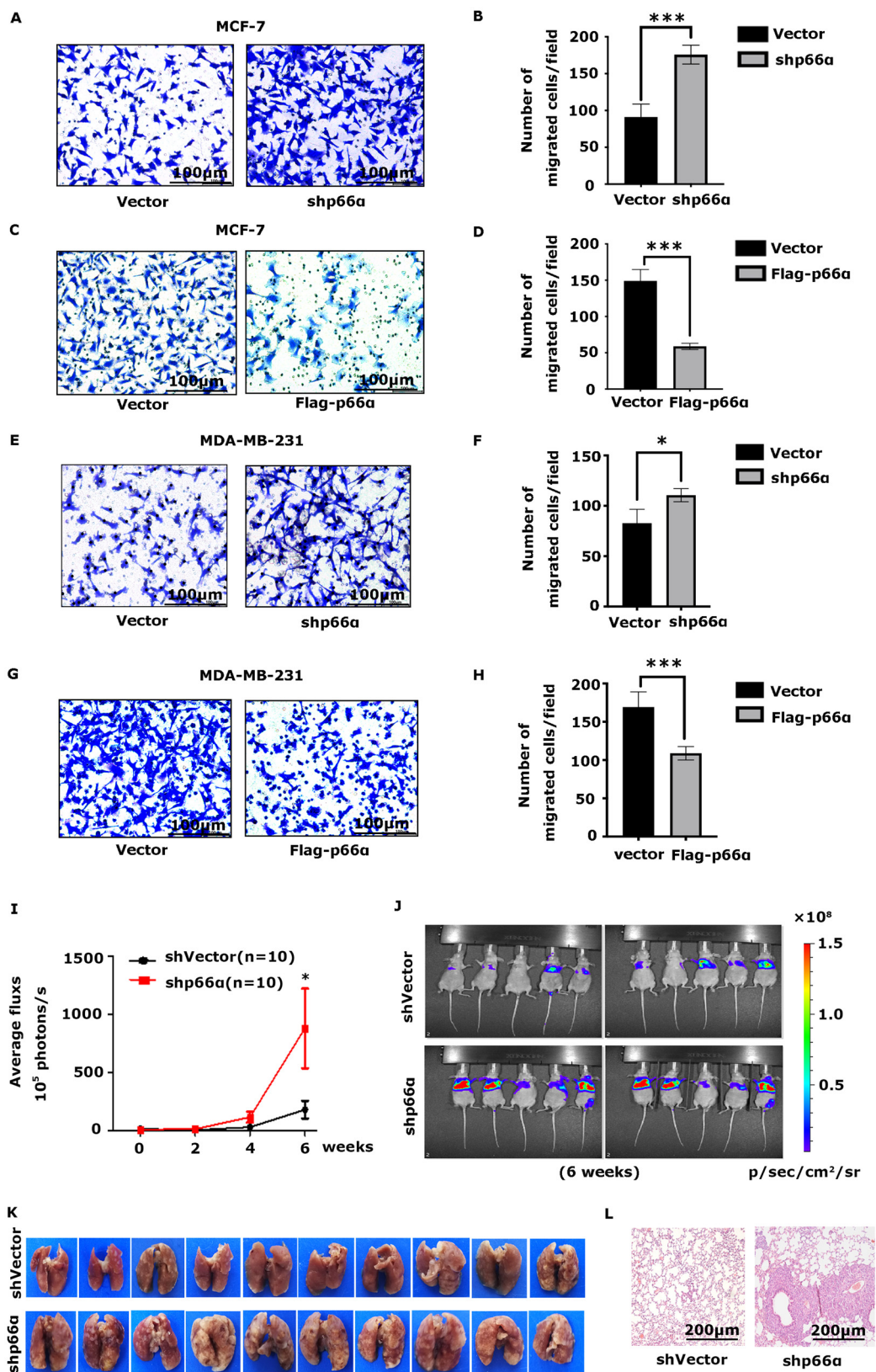


Figure 2. p66 α suppresses breast cancer cell migration and metastasis. (A) Transwell assays demonstrated that knockdown p66 α increased migration in MCF-7 cells (20 \times , scale bar: 100 μ m). (B) Quantification analyses of cell migration abilities of p66 α knockdown or vector MCF-7 cells. *** $p < 0.001$. (C) Transwell assays showed that an increase in p66 α levels reduced migration in MCF-7 cells

(20 \times , scale bar: 100 μ m). (D) Quantification analyses of cell migration abilities of MCF-7 cells overexpressing p66 α or vector. *** $p < 0.001$. (E) Depletion of p66 α increased cell migration in MDA-MB-231 cells. (20 \times , scale bar: 100 μ m). (F) Quantification analyses of cell migration abilities of p66 α knockdown MDA-MB-231 cells. * $p < 0.05$. (G) Transwell assays showed that an increase in p66 α levels reduced MDA-MB-231 cells migration (20 \times , scale bar: 100 μ m). (H) Quantification analyses of cell migration abilities of MDA-MB-231 cells overexpressing p66 α . *** $p < 0.001$. (I) MDA-MB-231-Luc cells stably expressing control vector or p66 α shRNA were injected into the tail vein of female nude mice. Luciferase signal intensities of lung metastases in each group ($n = 10$) were recorded every two weeks. * $p < 0.05$. (J) Representative luciferase signal images of lung metastases at the sixth week. (K) Representative images of metastatic nodules in the lung. (L) H&E staining of lung tissue in nude mice, which were injected cells as indicated. The metastatic foci in the shp66 α group were dramatically increased compared to the control group (10 \times , scale bar: 200 μ m).

3.4. The CR2 Domain of p66 α and the DNA-Binding Domain of p53 Are Essential for the Interaction

To identify regions in p66 α that are critical for the interaction between p66 α and p53, p66 α full-length or truncations were transiently co-expressed with GFP-p53 in HEK-293T cells. Co-IP assays demonstrated that CR1 only weakly bound p53, while the CR2 region robustly bound p53 (Figure 3E,F).

To determine the domains in p53 protein required for interacting with p66 α , the full length of GST-p53 and three truncated p53 proteins were purified and incubated with HA-p66 α protein prepared from HEK-293T cells. The co-precipitation experiments were performed by using GST beads, and the co-eluted HA-p66 α protein was examined by Western blot assays by using HA antibody. The truncation mutant consists of 100-291aa containing DNA-binding domain motif was capable of binding p66 α , which was comparable to that of the full-length p66 α , while the mutants comprising 1-99aa or 292-393aa of p53 failed to bind p66 α (Figure 3G,H). Taken together, the CR2 domain of p66 α and the DNA-binding domain (100-291aa) of p53 are essential for the interaction.

3.5. p66 α Promotes the Expression of p53 Target Genes

To determine if the p66 α -p53 interaction impacts p53 to regulate its target genes, we examined the expression of the known p53 target genes that control cell growth such as *BAX*, *GADD45A*, *NOXA*, and that control cell migration such as *PAI-1* in the MCF-7-shp66 α or vector control cells by qRT-PCR. Notably, depletion of p66 α decreased the expression of p53 target genes in MCF-7 cells (Figure 4A,B). Moreover, the increase in p66 α levels in MCF-7 cells promoted the expression of these targets (Figure 4C,D), which is dependent on the expression of p53 (Figure 4E,F). A similar effect of p66 α levels on the expression of the p53 target genes was observed in MDA-MB-231 cells (Figure 4G–L).

3.6. p66 α Promotes the Transactivity of p53 by Enhancing p53 Binding at Target Promoters

To verify the effects of p66 α on the transactivation ability of p53WT and p53R280K, we performed luciferase reporter assays with *BAX*-Luc or *NOXA*-Luc, which contained p53 responsive elements, respectively. Notably, both p53WT and p53R280K can transactivate *BAX* or *NOXA*, and a combination with p66 α markedly increased *BAX*- or *NOXA*-driven reporter activities (Figure 5A,B).

To examine whether p66 α affects the expression of p53, we detected the expression level of p53 in stable cells with knockdown or overexpression of p66 α . The results showed that p66 α did not affect the mRNA level of p53 (Figure S2A–C), nor did it affect the protein level of p53 (Figure S2D–F).

To determine the effects of p66 α on the DNA-binding activity of p53, we performed ChIP assays in MDA-MB-231-shVector and MDA-MB-231-shp66 α cells using antibodies specific to p53, and the enriched target DNA fragments were amplified by qPCR using primer sets flanking the functional p53 binding sites within target promoters. Depletion of p66 α significantly decreased the binding of p53 to target promoters including *BAX*, *NOXA*, *GADD45A*, and *PAI-1* (Figure 5C). Taken together, these results indicate that p66 α promotes the transactivity of p53 by enhancing p53 binding at target promoters.

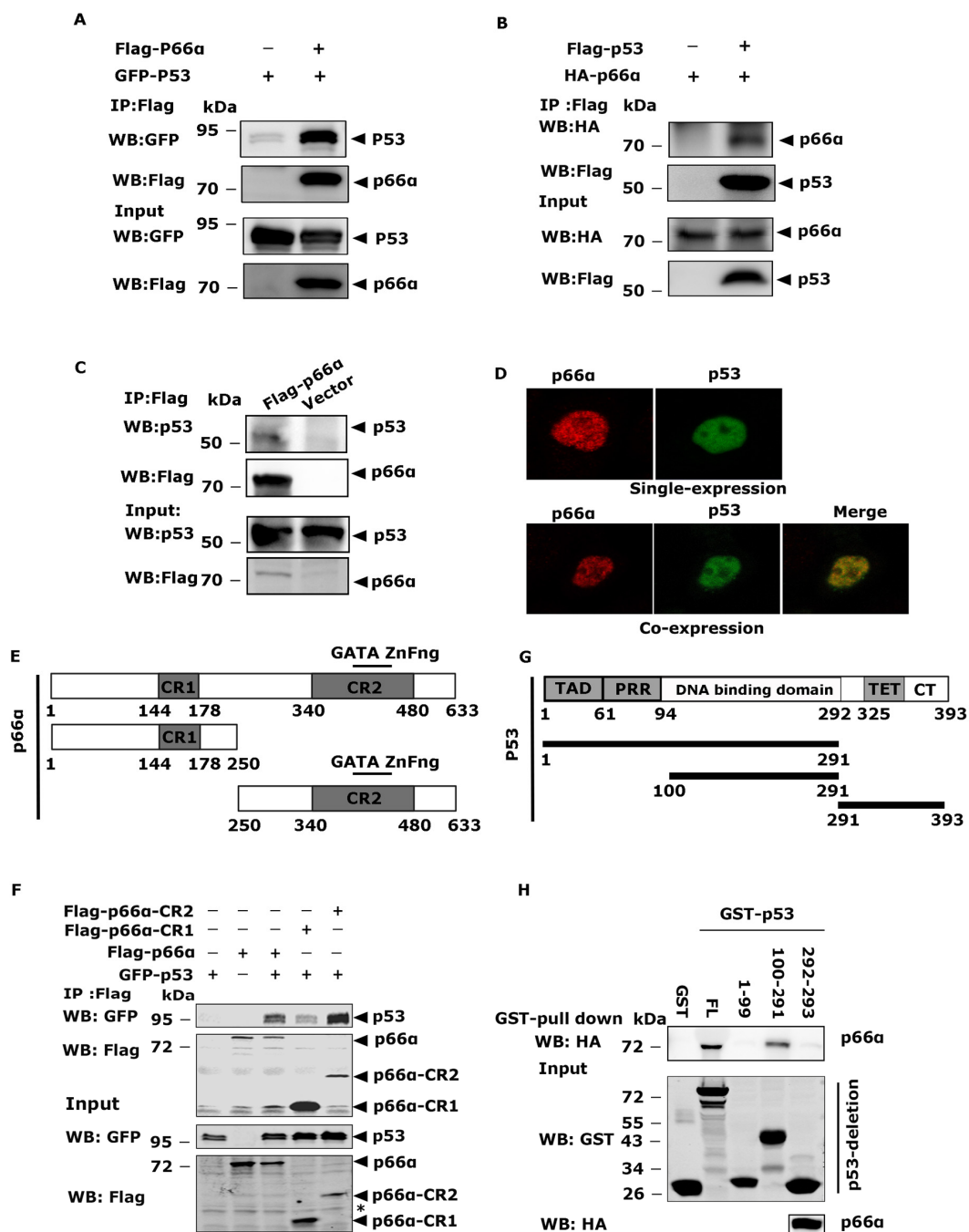


Figure 3. p66α directly binds the DNA-binding domain of p53. (A) The exogenously expressed Flag-p66α and GFP-p53 proteins interacted in HEK-293T cells. Immunoprecipitation was performed by using Flag M2 beads to enrich p66α, and Western blotting was probed with the anti-GFP antibody. (B) The exogenously expressed Flag-p53 and HA-p66α proteins interacted in HEK-293T cells. Immunoprecipitation was performed with Flag M2 beads to enrich p53, Western blotting was probed with the anti-HA antibody. (C) The exogenously expressed Flag-p66α and endogenous p53 proteins interacted in HEK293T cells. Immunoprecipitation was performed with Flag M2 beads, and Western blot was performed with monoclonal anti-p53 antibody. (D) Subcellular localization of p66α and p53 in HeLa cells. The plasmids encoding Flag-p66α and GFP-p53 were transiently transfected into HeLa cells, and the immunofluorescent images were taken with confocal microscopy. (E) Diagrams of full-length p66α and p66α deletion mutants. The CR1 and CR2 are the highly conserved regions in p66α. The CR2 domain contains a GATA-type zinc finger motif. (F) p53 mainly interacted with the CR2 domain of p66α, but there was also a weak interaction between p53 and CR1 domain. The asterisk “*” means nonspecific bands. (G) Diagrams of full-length p53 and p53 deletion mutants. (H) The region between 100 and 291 amino acid residues of p53 bound p66α. In vitro translated p66α protein was subjected to GST pull-down assays using the purified GST fusion p53 proteins.

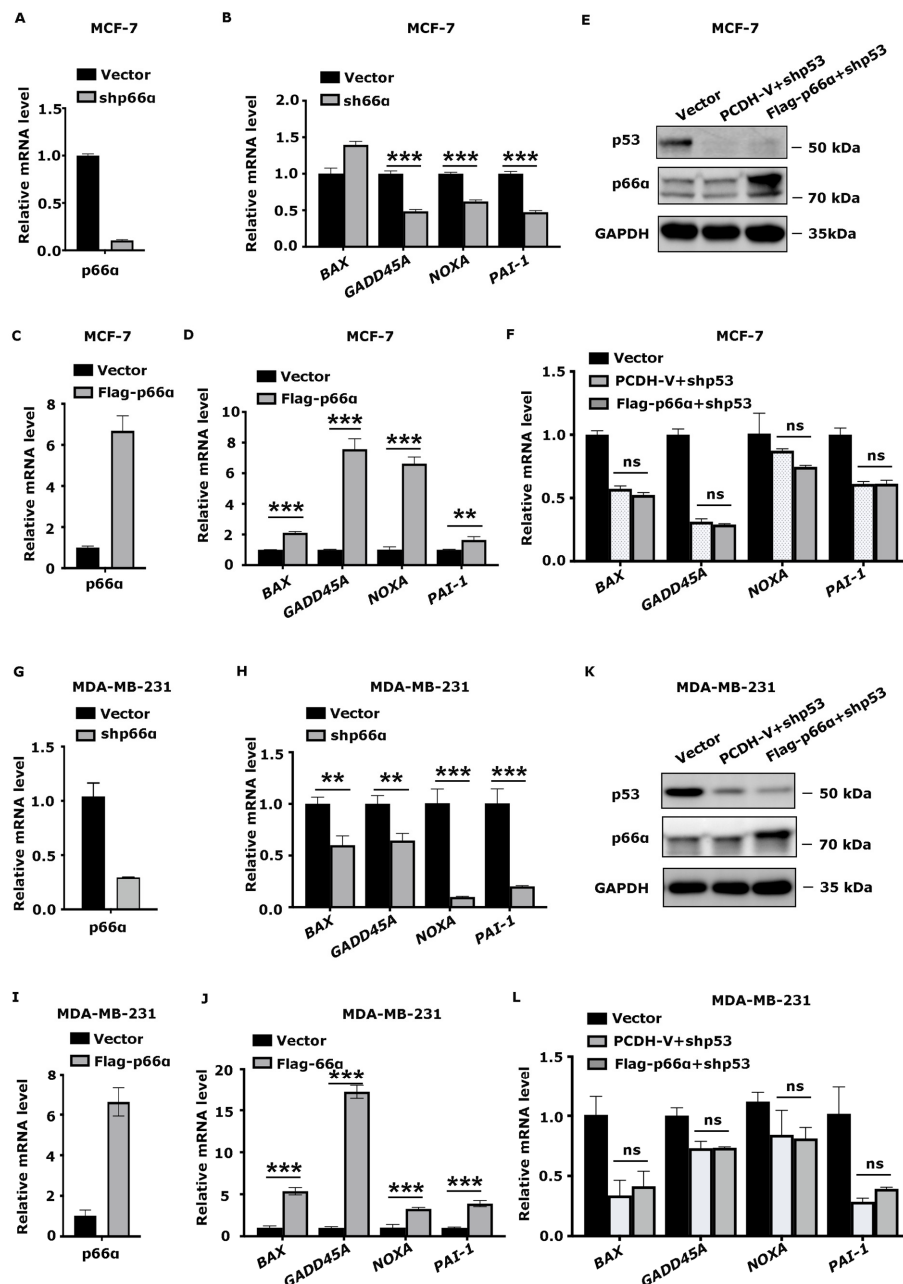


Figure 4. p66 α promotes the expression of transactivated p53 target genes via p53. (A) qRT-PCR assays verified the mRNA level of p66 α in MCF-7 shVector and shp66 α cells. (B) The repression of p66 α decreased the mRNA level of p53 target genes in MCF-7 cells. *** $p < 0.001$. (C) qRT-PCR assays verified the mRNA level of p66 α in Flag-p66 α overexpressing MCF-7 cells. (D) Overexpression of p66 α increased the mRNA levels of p53 downstream genes in MCF-7 cells. ** $p < 0.01$, *** $p < 0.001$. (E) Western blot assays verified the protein levels of p53, p66 α in p66 α overexpressing MCF-7 cells after the depression of p53. (F) qRT-PCR assays of the mRNA level of p53 downstream genes after the depression of p53 in p66 α overexpressing MCF-7 cells. “ns” indicates no significant difference ($p > 0.05$). (G) qRT-PCR assays verified the mRNA level of p66 α in MDA-MB-231 shVector and shp66 α cells. (H) Repression of p66 α decreased the mRNA level of p53 downstream genes in MDA-MB-231 cells. ** $p < 0.01$, *** $p < 0.001$. (I) qRT-PCR assays verified the mRNA level of p66 α in MDA-MB-231 Flag-p66 α overexpressing cells. (J) Overexpressing p66 α induced the mRNA level of p53 downstream genes. *** $p < 0.001$. (K) Western blot assays verified the protein levels of p53, p66 α in p66 α overexpressing MDA-MB-231 cells after the depression of p53. (L) qRT-PCR assays of the mRNA level of p53 downstream genes after the depression of p53 in p66 α overexpressing MDA-MB-231 cells. “ns” indicates no significant difference ($p > 0.05$). All data were shown as mean \pm S.D. from three independent experiments.

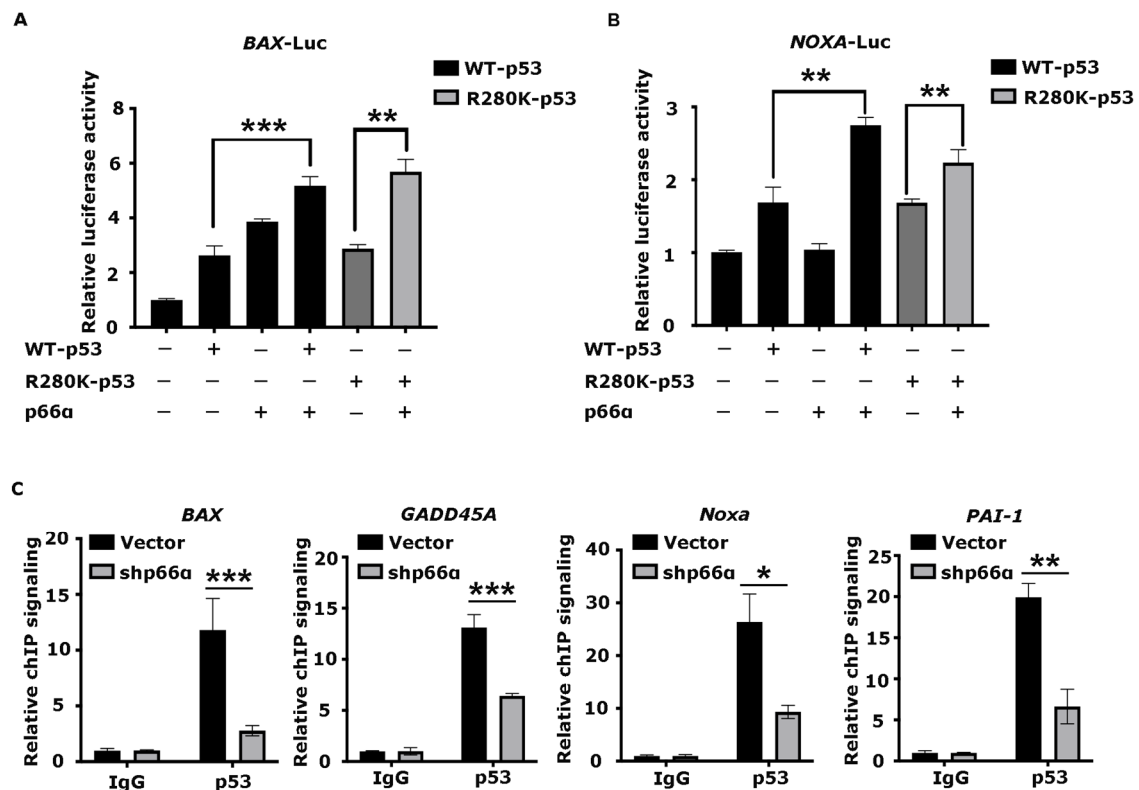


Figure 5. p66 α promotes the transactivity of p53 by enhancing p53 binding at target promoters (A) Luciferase assays were performed in HEK-293T cells knocking down of p53. The value was normalized to β -gal. Both p53WT and p53R280K synergistically worked with p66 α to transactivate the BAX promoter. (B) Luciferase assays showed that both p53WT and p53R280K synergistically worked with p66 α to transactivate the NOXA promoter. (C) ChIP assays were performed in MDA-MB-231-shp66 α and shVector cells using an antibody specific to p53. The enriched DNA fragments were amplified by qRT-PCR assays. * $p < 0.05$, ** $p < 0.01$, *** $p < 0.001$. All data were shown as mean \pm S.D. from three independent experiments.

3.7. High Expression of p66 α and p53 Is Positively Correlated and Predicts Good Prognosis in Breast Cancer

To determine the clinical relevance of p66 α and p53, we analyzed a Kaplan-Meier plotter database and found that high expression of p53 also predicted good prognoses in patients with breast tumors (Figure 6A). Moreover, the expression of p66 α and p53 have a significant correlation in breast cancer samples (Figure 6B).

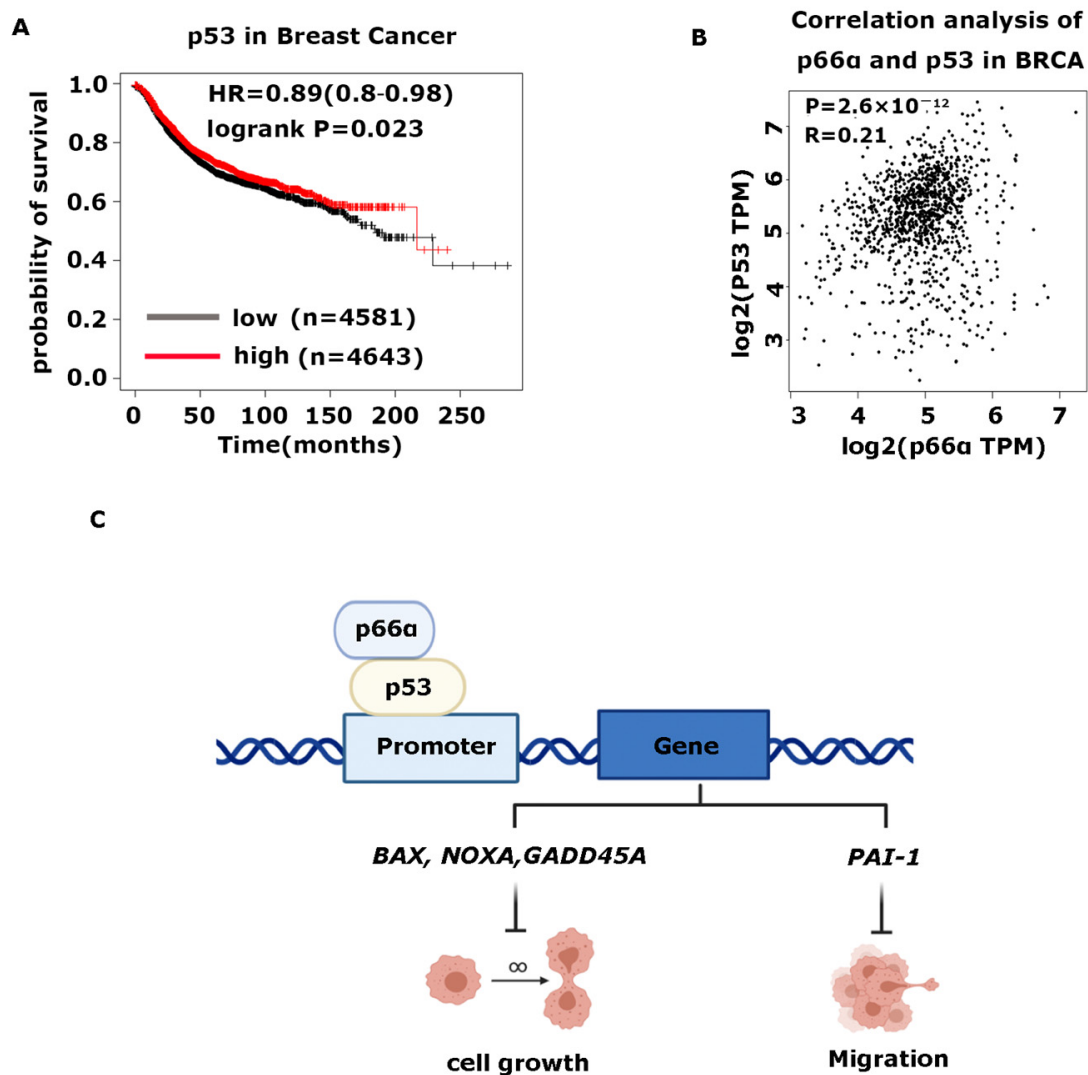


Figure 6. High expression of p66 α and p53 is positively correlated with and predicts a good prognosis in breast cancer. (A) Kaplan-Meier plot of the relapse-free survival of patients with breast cancer in whole data sets stratified by p53 expression. (B) Scatter plot showed that p66 α and p53 were positively correlated in breast cancer. The p value was calculated via Pearson's ranking correlation coefficient analysis. BRCA: breast invasive carcinoma (TCGA database). TPM: Transcripts Per Kilobase of exon per Million mapped reads. (C) Schematic model for p66 α mediated p53 transactivating genes expression. p66 α interacted with p53 and promoted the transcriptional activation ability of p53 by enhancing p53 binding in target promoters, including genes that control cell growth, such as *BAX*, *GADD45A*, and *NOXA*, and that control cell migration such as *PAI-1*.

4. Discussion

4.1. p66 α Functions as a Tumor Suppressor of Breast Cancer Cells

Breast cancer is one of the most common cancers in women, which has a mortality-to-incidence ratio of 15% and alone accounts for 30% of female cancers [51]. As a heterogeneous malignancy, it could be divided into three categories according to molecular features, including hormone-positive subtype expressing estrogen receptor (ER+) or progesterone receptor (PR+), HER2-positive subtype expressing human epidermal receptor 2 (HER2+), and triple-negative breast cancer (TNBC) (ER-, PR-, HER2-) [52]. The TNBC treatment is the most challenging within breast cancer for its higher aggressive feature and lack of molecular targets [53–55], although there are a large number of tumor suppressor genes encoding proteins that inhibit cell transformation in breast cancer, such as *TP53*, *Rb1*, *PTEN*, *BRCA1/2*, *CDKN1B*, *CDKN2A*, etc.

In this study, we demonstrate that p66 α functions as a tumor suppressor that can inhibit breast cancer cell growth and migration. Expression of p66 α can inhibit growth and migration of breast cancer cells MCF-7 and MDA-MB-231, as well as normal breast cells MCF-10A. Mechanistically, p66 α functions as a novel co-activator of p53 to induce its target gene expression, and p66 α promotes the transactivity of p53 by enhancing p53 binding at target promoters such as *BAX*, *NOXA*, *GADD45A*, and *PAI-1*, resulting in inhibition of cell growth and migration. Moreover, breast cancer patients having a higher level of p66 α exhibit better prognosis. Taken together, our findings suggest that p66 α could be a target for new strategies in the treatment of breast cancers.

4.2. p66 α Functions as a Potent Co-Activator of p53 by Enhancing Its DNA-Binding Activity

Although p66 α harbors a GATA motif within its CR2 region, there is no evidence to show that p66 α can directly bind DNA sequences; rather, p66 α acts like an adapter or a scaffold to participate in assembly of various protein complexes. Thus, the molecular mechanism by which p66 α enhances the DNA-binding and transcriptional activity of p53 remains elusive and definitely needs to be explored further. For example, identifying the protein partners that associate with p53/p66 α complex will provide new clues.

Another interesting observation is that p66 α can enhance p53 target gene expression in MDA-MB-231 cells in a p53-dependent manner, since the p53 protein in MDA-MB-231 cells harbor the R280K mutation. R280K resides in the DNA-binding domain and results in impaired DNA-binding activity of p53 [56,57]. We found the p53R280K is also enriched at the promoters of target genes including *BAX*, *NOXA*, *GADD45A*, and *PAI-1* in MDA-MB-231 cells. Moreover, the luciferase reporter assays on promoters of *BAX* and *NOXA* showed that both p53 WT and R280K alone can induce their promoter activities, and adding p66 α can further induce these promoter-luc activities.

We reasoned that this may be explained by at least two possible mechanisms: (1) p53R280K mutant still retains DNA-binding activity. Malcikova reported that p53R280K lost most of its binding ability to the *CDKN1A* and retained about 35% binding ability to the *BAX* gene [58]. In another study, the DNA-binding ability of p53R280K to the *GADD45A* gene was reduced, but not completely lost [59]. (2) MDA-MB-231 cells express a relatively higher level of p66 α protein compared to MCF-7 and MCF-10A cells. Our data show that p66 α can enhance the DNA-binding activity of p53 to its target promoters. The binding activities of p53R280K to its target promoters in MDA-MB-231 cells may be attributed to p66 α , which may overcome the effect of the mutation.

Supplementary Materials: The following are available online at <https://www.mdpi.com/article/10.3390/cells10123593/s1>, Figure S1: p66 α suppresses cell growth and migration in MCF-10A cell line, Figure S2: The protein and mRNA level of p53 is not affected by p66 α expression or knockdown, Table S1: A list of primer sequences applied in qRT-PCR, Table S2: A list of primer sequences applied in ChIP qRT-PCR.

Author Contributions: Conceptualization, Z.H., X.Z.; methodology, Q.Z., Y.Z., J.Z., D.Z., M.L., H.Y., H.Z., J.W., L.S., X.Z., Y.Y.; software, Q.Z., X.Z.; validation, Q.Z., Y.Y., X.Z.; formal analysis, Q.Z., X.Z.; writing—review and editing, X.Z., Y.Y., Z.H.; visualization, Q.Z., X.Z.; supervision, Y.Y., Z.H.; project administration, Z.H., X.Z.; funding acquisition, Y.Z., Z.H. All authors have read and agreed to the published version of the manuscript.

Funding: This research was funded by the National Science Foundation of China (81402177, 81903003); the Shandong Provincial Natural Science Foundation (ZR2021ZD16); the State Key Laboratory of Oncogenes and Related Genes of China; and the Key Laboratory of Cell Differentiation and Apoptosis of the Chinese Ministry of Education.

Institutional Review Board Statement: Animal experiments were conducted in accordance with institutional guidelines approved by the Institutional Animal Care and Use Committee (IACUC) of Shanghai Jiao Tong University School of Medicine (approval code: A-2019-031; approval date: 2019).

Informed Consent Statement: Not applicable.

Data Availability Statement: All data generated or analyzed during this study are included in this published article.

Acknowledgments: We thank Reiner Renkawitz at the Genetisches Institut Justus-Liebig-Universität and Jing Yi at the Shanghai Jiaotong University School of Medicine for providing plasmids. We are also grateful for the support from the Hongqiao International Institute of Medicine, Tongren Hospital/Faculty of Basic Medicine, Shanghai Jiaotong University School of Medicine.

Conflicts of Interest: The authors declare no conflict of interest.

References

1. Brackertz, M.; Boeke, J.; Zhang, R.; Renkawitz, R. Two highly related p66 proteins comprise a new family of potent transcriptional repressors interacting with MBD2 and MBD3. *J. Biol. Chem.* **2002**, *277*, 40958–40966. [[CrossRef](#)] [[PubMed](#)]
2. Eom, K.S.; Cheong, J.S.; Lee, S.J. Structural Analyses of Zinc Finger Domains for Specific Interactions with DNA. *J. Microbiol. Biotechnol.* **2016**, *26*, 2019–2029. [[CrossRef](#)]
3. Miller, J.; McLachlan, A.D.; Klug, A. Repetitive zinc-binding domains in the protein transcription factor IIIA from *Xenopus* oocytes. *EMBO J.* **1985**, *4*, 1609–1614. [[CrossRef](#)]
4. Schulz, R.A. GATA transcription factors in heart and blood cell development and disease. *Semin. Cell Dev. Biol.* **2005**, *16*, 69. [[CrossRef](#)]
5. Patient, R.K.; McGhee, J.D. The GATA family (vertebrates and invertebrates). *Curr. Opin. Genet. Dev.* **2002**, *12*, 416–422. [[CrossRef](#)]
6. Omichinski, J.G.; Clore, G.M.; Schaad, O.; Felsenfeld, G.; Trainor, C.; Appella, E.; Stahl, S.J.; Gronenborn, A.M. NMR structure of a specific DNA complex of Zn-containing DNA binding domain of GATA-1. *Science* **1993**, *261*, 438–446. [[CrossRef](#)] [[PubMed](#)]
7. Merika, M.; Orkin, S.H. DNA-binding specificity of GATA family transcription factors. *Mol. Cell. Biol.* **1993**, *13*, 3999–4010. [[CrossRef](#)]
8. Kowalski, K.; Liew, C.K.; Matthews, J.M.; Gell, D.A.; Crossley, M.; Mackay, J.P. Characterization of the conserved interaction between GATA and FOG family proteins. *J. Biol. Chem.* **2002**, *277*, 35720–35729. [[CrossRef](#)] [[PubMed](#)]
9. Yang, H.Y.; Evans, T. Distinct roles for the two cGATA-1 finger domains. *Mol. Cell Biol.* **1992**, *12*, 4562–4570. [[CrossRef](#)] [[PubMed](#)]
10. Brackertz, M.; Gong, Z.; Leers, J.; Renkawitz, R. p66alpha and p66beta of the Mi-2/NuRD complex mediate MBD2 and histone interaction. *Nucleic Acids Res.* **2006**, *34*, 397–406. [[CrossRef](#)] [[PubMed](#)]
11. Torchy, M.P.; Hamiche, A.; Klaholz, B.P. Structure and function insights into the NuRD chromatin remodeling complex. *Cell Mol. Life Sci.* **2015**, *72*, 2491–2507. [[CrossRef](#)]
12. Ding, X.; Liu, S.; Tian, M.; Zhang, W.; Zhu, T.; Li, D.; Wu, J.; Deng, H.; Jia, Y.; Xie, W.; et al. Activity-induced histone modifications govern Neurexin-1 mRNA splicing and memory preservation. *Nat. Neurosci.* **2017**, *20*, 690–699. [[CrossRef](#)] [[PubMed](#)]
13. Kim, M.Y.; Kim, J.S.; Son, S.H.; Lim, C.S.; Eum, H.Y.; Ha, D.H.; Park, M.A.; Baek, E.J.; Ryu, B.Y.; Kang, H.C.; et al. Mbd2-CP2c loop drives adult-type globin gene expression and definitive erythropoiesis. *Nucleic Acids Res.* **2018**, *46*, 4933–4949. [[CrossRef](#)] [[PubMed](#)]
14. Mor, N.; Rais, Y.; Sheban, D.; Peles, S.; Aguilera-Castrejon, A.; Zviran, A.; Elinger, D.; Viukov, S.; Geula, S.; Krupalnik, V.; et al. Neutralizing Gata2a-Chd4-Mbd3/NuRD Complex Facilitates Deterministic Induction of Naive Pluripotency. *Cell Stem Cell* **2018**, *23*, 412–425. [[CrossRef](#)] [[PubMed](#)]
15. Pergola, G.; Di Carlo, P.; D'Ambrosio, E.; Gelao, B.; Fazio, L.; Papalino, M.; Monda, A.; Scozia, G.; Pietrangelo, B.; Attrotto, M.; et al. DRD2 co-expression network and a related polygenic index predict imaging, behavioral and clinical phenotypes linked to schizophrenia. *Transl. Psychiatry* **2017**, *7*, e1006. [[CrossRef](#)] [[PubMed](#)]
16. Torretta, S.; Rampino, A.; Basso, M.; Pergola, G.; Di Carlo, P.; Shin, J.H.; Kleinman, J.E.; Hyde, T.M.; Weinberger, D.R.; Masellis, R.; et al. NURR1 and ERR1 Modulate the Expression of Genes of a DRD2 Coexpression Network Enriched for Schizophrenia Risk. *J. Neurosci.* **2020**, *40*, 932–941. [[CrossRef](#)] [[PubMed](#)]
17. Wang, Z.; Kang, J.; Deng, X.; Guo, B.; Wu, B.; Fan, Y. Knockdown of GATAD2A suppresses cell proliferation in thyroid cancer in vitro. *Oncol. Rep.* **2017**, *37*, 2147–2152. [[CrossRef](#)] [[PubMed](#)]
18. Whitton, L.; Apostolova, G.; Rieder, D.; Dechant, G.; Rea, S.; Donohoe, G.; Morris, D.W. Genes regulated by SATB2 during neurodevelopment contribute to schizophrenia and educational attainment. *PLoS Genet.* **2018**, *14*, e1007515. [[CrossRef](#)]
19. Yu, T.; Ding, Y.; Zhang, Y.; Liu, Y.; Li, Y.; Lei, J.; Zhou, J.; Song, S.; Hu, B. Circular RNA GATAD2A promotes H1N1 replication through inhibiting autophagy. *Vet. Microbiol.* **2019**, *231*, 238–245. [[CrossRef](#)] [[PubMed](#)]
20. Zviran, A.; Mor, N.; Rais, Y.; Gingold, H.; Peles, S.; Chomsky, E.; Viukov, S.; Buenrostro, J.D.; Scognamiglio, R.; Weinberger, L.; et al. Deterministic Somatic Cell Reprogramming Involves Continuous Transcriptional Changes Governed by Myc and Epigenetic-Driven Modules. *Cell Stem Cell* **2019**, *24*, 328–341.e329. [[CrossRef](#)]
21. Gnanapragasam, M.N.; Scarsdale, J.N.; Amaya, M.L.; Webb, H.D.; Desai, M.A.; Walavalkar, N.M.; Wang, S.Z.; Zu Zhu, S.; Ginder, G.D.; Williams, D.C., Jr. p66Alpha-MBD2 coiled-coil interaction and recruitment of Mi-2 are critical for globin gene silencing by the MBD2-NuRD complex. *Proc. Natl. Acad. Sci. USA* **2011**, *108*, 7487–7492. [[CrossRef](#)]
22. Spruijt, C.G.; Luijsterburg, M.S.; Menafra, R.; Lindeboom, R.G.; Jansen, P.W.; Edupuganti, R.R.; Baltissen, M.P.; Wiegant, W.W.; Voelker-Albert, M.C.; Matarese, F.; et al. ZMYND8 Co-localizes with NuRD on Target Genes and Regulates Poly(ADP-Ribose)-Dependent Recruitment of GATAD2A/NuRD to Sites of DNA Damage. *Cell Rep.* **2016**, *17*, 783–798. [[CrossRef](#)] [[PubMed](#)]

23. Liang, Y.; Zhang, X.; Liu, Y.; Wang, L.; Ye, Y.; Tan, X.; Pu, J.; Zhang, Q.; Bao, X.; Wei, X.; et al. GATA zinc finger domain-containing protein 2A (GATAD2A) deficiency reactivates fetal haemoglobin in patients with beta-thalassaemia through impaired formation of methyl-binding domain protein 2 (MBD2)-containing nucleosome remodelling and deacetylation (NuRD) complex. *Br. J. Haematol.* **2021**, *193*, 1220–1227. [[CrossRef](#)]
24. Gong, Z.; Brackertz, M.; Renkawitz, R. SUMO modification enhances p66-mediated transcriptional repression of the Mi-2/NuRD complex. *Mol. Cell Biol.* **2006**, *26*, 4519–4528. [[CrossRef](#)]
25. Kantor, B.; Makedonski, K.; Shemer, R.; Razin, A. Expression and localization of components of the histone deacetylases multiprotein repressory complexes in the mouse preimplantation embryo. *Gene Expr. Patterns* **2003**, *3*, 697–702. [[CrossRef](#)]
26. Marino, S.; Nusse, R. Mutants in the mouse NuRD/Mi2 component P66alpha are embryonic lethal. *PLoS ONE* **2007**, *2*, e519. [[CrossRef](#)]
27. Xin, J.; Zhang, Z.; Su, X.; Wang, L.; Zhang, Y.; Yang, R. Epigenetic Component p66a Modulates Myeloid-Derived Suppressor Cells by Modifying STAT3. *J. Immunol.* **2017**, *198*, 2712–2720. [[CrossRef](#)]
28. Kar, S.P.; Beesley, J.; Amin Al Olama, A.; Michailidou, K.; Tyrer, J.; Kote-Jarai, Z.; Lawrenson, K.; Lindstrom, S.; Ramus, S.J.; Thompson, D.J.; et al. Genome-Wide Meta-Analyses of Breast, Ovarian, and Prostate Cancer Association Studies Identify Multiple New Susceptibility Loci Shared by at Least Two Cancer Types. *Cancer Discov.* **2016**, *6*, 1052–1067. [[CrossRef](#)]
29. Lu, D.; Song, J.; Lu, Y.; Fall, K.; Chen, X.; Fang, F.; Landén, M.; Hultman, C.M.; Czene, K.; Sullivan, P.; et al. A shared genetic contribution to breast cancer and schizophrenia. *Nat. Commun.* **2020**, *11*, 1–10. [[CrossRef](#)] [[PubMed](#)]
30. Shu, K.X.; Li, B.; Wu, L.X. The p53 network: p53 and its downstream genes. *Colloids Surf. B Biointerfaces* **2007**, *55*, 10–18. [[CrossRef](#)] [[PubMed](#)]
31. Vogelstein, B.; Lane, D.; Levine, A.J. Surfing the p53 network. *Nature* **2000**, *408*, 307–310. [[CrossRef](#)] [[PubMed](#)]
32. Prives, C.; Hall, P.A. The p53 pathway. *J. Pathol.* **1999**, *187*, 112–126. [[CrossRef](#)]
33. Agarwal, M.L.; Agarwal, A.; Taylor, W.R.; Stark, G.R. p53 controls both the G2/M and the G1 cell cycle checkpoints and mediates reversible growth arrest in human fibroblasts. *Proc. Natl. Acad. Sci. USA* **1995**, *92*, 8493–8497. [[CrossRef](#)]
34. Kruiswijk, F.; Labuschagne, C.F.; Vousden, K.H. p53 in survival, death and metabolic health: A lifeguard with a licence to kill. *Nat. Rev. Mol. Cell Biol.* **2015**, *16*, 393–405. [[CrossRef](#)] [[PubMed](#)]
35. Muller, P.A.; Vousden, K.H.; Norman, J.C. p53 and its mutants in tumor cell migration and invasion. *J. Cell. Biol.* **2011**, *192*, 209–218. [[CrossRef](#)] [[PubMed](#)]
36. Powell, E.; Piwnica-Worms, D.; Piwnica-Worms, H. Contribution of p53 to metastasis. *Cancer Discov.* **2014**, *4*, 405–414. [[CrossRef](#)] [[PubMed](#)]
37. Teodoro, J.G.; Evans, S.K.; Green, M.R. Inhibition of tumor angiogenesis by p53: A new role for the guardian of the genome. *J. Mol. Med.* **2007**, *85*, 1175–1186. [[CrossRef](#)]
38. Walerych, D.; Napoli, M.; Collavin, L.; Del Sal, G. The rebel angel: Mutant p53 as the driving oncogene in breast cancer. *Carcinogenesis* **2012**, *33*, 2007–2017. [[CrossRef](#)] [[PubMed](#)]
39. Petitjean, A.; Mathe, E.; Kato, S.; Ishioka, C.; Tavtigian, S.V.; Hainaut, P.; Olivier, M. Impact of mutant p53 functional properties on TP53 mutation patterns and tumor phenotype: Lessons from recent developments in the IARC TP53 database. *Hum. Mutat.* **2007**, *28*, 622–629. [[CrossRef](#)]
40. Resnick, M.A.; Inga, A. Functional mutants of the sequence-specific transcription factor p53 and implications for master genes of diversity. *Proc. Natl. Acad. Sci. USA* **2003**, *100*, 9934–9939. [[CrossRef](#)] [[PubMed](#)]
41. Jordan, J.J.; Inga, A.; Conway, K.; Edmiston, S.; Carey, L.A.; Wu, L.; Resnick, M.A. Altered-Function p53 Missense Mutations Identified in Breast Cancers Can Have Subtle Effects on Transactivation. *Mol. Cancer Res.* **2010**, *8*, 701–716. [[CrossRef](#)]
42. Kato, S.; Han, S.Y.; Liu, W.; Otsuka, K.; Shibata, H.; Kanamaru, R.; Ishioka, C. Understanding the function-structure and function-mutation relationships of p53 tumor suppressor protein by high-resolution missense mutation analysis. *Proc. Natl. Acad. Sci. USA* **2003**, *100*, 8424–8429. [[CrossRef](#)] [[PubMed](#)]
43. Kim, E.; Deppert, W. Transcriptional activities of mutant p53: When mutations are more than a loss. *J. Cell Biochem.* **2004**, *93*, 878–886. [[CrossRef](#)] [[PubMed](#)]
44. Weisz, L.; Oren, M.; Rotter, V. Transcription regulation by mutant p53. *Oncogene* **2007**, *26*, 2202–2211. [[CrossRef](#)]
45. Fontemaggi, G.; Dell’Orso, S.; Trisciuglio, D.; Shay, T.; Melucci, E.; Fazi, F.; Terrenato, I.; Mottolise, M.; Muti, P.; Domany, E.; et al. The execution of the transcriptional axis mutant p53, E2F1 and ID4 promotes tumor neo-angiogenesis. *Nat. Struct. Mol. Biol.* **2009**, *16*, U1086–U1111. [[CrossRef](#)]
46. Girardini, J.E.; Napoli, M.; Piazza, S.; Rustighi, A.; Marotta, C.; Radaelli, E.; Capaci, V.; Jordan, L.; Quinlan, P.; Thompson, A.; et al. A Pin1/Mutant p53 Axis Promotes Aggressiveness in Breast Cancer. *Cancer Cell* **2011**, *20*, 79–91. [[CrossRef](#)] [[PubMed](#)]
47. Roger, L.; Jullien, L.; Gire, V.; Roux, P. Gain of oncogenic function of p53 mutants regulates E-cadherin expression uncoupled from cell invasion in colon cancer cells. *J. Cell Sci.* **2010**, *123*, 1295–1305. [[CrossRef](#)] [[PubMed](#)]
48. Hou, Z.; Peng, H.; Ayyanathan, K.; Yan, K.P.; Langer, E.M.; Longmore, G.D.; Rauscher, F.J., 3rd. The LIM protein AJUBA recruits protein arginine methyltransferase 5 to mediate SNAIL-dependent transcriptional repression. *Mol. Cell Biol.* **2008**, *28*, 3198–3207. [[CrossRef](#)] [[PubMed](#)]
49. Hou, Z.; Peng, H.; White, D.E.; Negorev, D.G.; Maul, G.G.; Feng, Y.; Longmore, G.D.; Waxman, S.; Zelent, A.; Rauscher, F.J., 3rd. LIM protein Ajuba functions as a nuclear receptor corepressor and negatively regulates retinoic acid signaling. *Proc. Natl. Acad. Sci. USA* **2010**, *107*, 2938–2943. [[CrossRef](#)]

50. Zhang, Y.H.; Zou, X.Q.; Qian, W.L.; Weng, X.L.; Zhang, L.; Zhang, L.; Wang, S.; Cao, X.; Ma, L.; Wei, G.; et al. Enhanced PAPSS2/VCAN sulfation axis is essential for Snail-mediated breast cancer cell migration and metastasis. *Cell Death Differ.* **2019**, *26*, 565–579. [[CrossRef](#)]
51. Loibl, S.; Poortmans, P.; Morrow, M.; Denkert, C.; Curigliano, G. Breast cancer. *Lancet* **2021**, *397*, 1750–1769. [[CrossRef](#)]
52. Barzaman, K.; Karami, J.; Zarei, Z.; Hosseinzadeh, A.; Kazemi, M.H.; Moradi-Kalbolandi, S.; Safari, E.; Farahmand, L. Breast cancer: Biology, biomarkers, and treatments. *Int. Immunopharmacol.* **2020**, *84*. [[CrossRef](#)] [[PubMed](#)]
53. Avery-Kiejda, K.A.; Mathe, A.; Scott, R.J. Genome-wide miRNA, gene and methylation analysis of triple negative breast cancer to identify changes associated with lymph node metastases. *Genom. Data* **2017**, *14*, 1–4. [[CrossRef](#)]
54. Sporikova, Z.; Koudelakova, V.; Trojanec, R.; Hajduch, M. Genetic Markers in Triple-Negative Breast Cancer. *Clin. Breast Cancer* **2018**, *18*, E841–E850. [[CrossRef](#)]
55. Howard, F.M.; Olopade, O.I. Epidemiology of Triple-Negative Breast Cancer A Review. *Cancer J.* **2021**, *27*, 8–16. [[CrossRef](#)] [[PubMed](#)]
56. Cho, Y.; Gorina, S.; Jeffrey, P.D.; Pavletich, N.P. Crystal structure of a p53 tumor suppressor-DNA complex: Understanding tumorigenic mutations. *Science* **1994**, *265*, 346–355. [[CrossRef](#)] [[PubMed](#)]
57. Wright, J.D.; Noskov, S.Y.; Lim, C. Factors governing loss and rescue of DNA binding upon single and double mutations in the p53 core domain. *Nucleic Acids Res.* **2002**, *30*, 1563–1574. [[CrossRef](#)] [[PubMed](#)]
58. Malcikova, J.; Tichy, B.; Damborsky, J.; Kabathova, J.; Trbusek, M.; Mayer, J.; Pospisilova, S. Analysis of the DNA-binding activity of p53 mutants using functional protein microarrays and its relationship to transcriptional activation. *Biol. Chem.* **2010**, *391*, 197–205. [[CrossRef](#)] [[PubMed](#)]
59. Boutell, J.M.; Hart, D.J.; Godber, B.L.; Kozlowski, R.Z.; Blackburn, J.M. Functional protein microarrays for parallel characterisation of p53 mutants. *Proteomics* **2004**, *4*, 1950–1958. [[CrossRef](#)] [[PubMed](#)]